PHYSICAL REVIEW A VOLUME 48, NUMBER 2 AUGUST 1993

Ion-collision spectrometric study of the dissociation dynamics of $S_2{}^+$ and CS^+ radicals

G. Ravindra Kumar, Latika Menon, and D. Mathur
Tata Institute of Fundamental Research, Homi Bhabha Road, Bombay 400 005, India

(Received 21 January 1993; revised manuscript received 14 April 1993)

Collision-induced dissociation experiments on ground-state $S_2{}^+$ and CS^+ have been carried out using a crossed-beam ion translational energy spectrometer with a very high angular resolution ($\leq 10^{-4}$ rad). The distributions of kinetic energies released upon dissociations $S_2{}^+ \rightarrow S^+ + S$, $CS^+ \rightarrow S^+ + C$, and $CS^+ \rightarrow C^+ + S$ in 3-keV collisions with N_2 have been measured; dissociation channels have been identified with the aid of computer simulations of trajectories through the apparatus of ions possessing different center-of-mass kinetic-energy release ($K_{\mathrm{c.m.}}$) components. In the case of S^+ formation from $S_2{}^+$, dissociation occurs via excitation to repulsive $S_2{}^{+*}$ electronic states, giving rise to $K_{\mathrm{c.m.}}$ components of 1.5 and 2.0 eV; lower $K_{\mathrm{c.m.}}$ values (0 and 0.3 eV) are obtained upon dissociation of a bound excited state of $S_2{}^+$ by a curve-crossing mechanism. Dissociation of CS^+ occurs via rotational resonances, giving rise to narrow, symmetrical structure in the S^+ translational energy spectrum; direct dissociation also occurs which yields relatively high $K_{\mathrm{c.m.}}$ values due to the breaking of the strong $C\equiv S$ triple bond. The $CS^+ \rightarrow C^+ + S$ channel is considerably weaker.

PACS number(s): 34.20.−b, 35.20.Gs, 34.50.Gb,

I. INTRODUCTION

Studies of neutral and ionized sulfur-containing diatomic radicals have assumed increased importance in recent years due to the significant role these species play in combustion processes and as intermediaries in chemical transformation processes in low-temperature interstellar plasmas, in planetary and oxygen-rich stellar atmospheres, and in cometary environments [1]. Moreover, many of these radical species are also of intrinsic interest from the viewpoint of quantal descriptions of their molecular properties. For instance, the CS radical is notable in that its ionization spectrum cannot be predicted by one-electron single-particle theories of molecular structure. Whereas ultraviolet photoelectron spectra show four ionization bands [2], application of Koopman's theorem to results of conventional Hartree-Fock treatments of CS^+ lead to predictions of only three of the bands [3]. Green-function calculations [4] have indicated that inclusion of many-body corrections to Koopman's theorem is mandatory in order to obtain a satisfactory description of the ordering of molecular orbitals in the apparently simple diatomic ion CS^+.

Experimental studies of the dissociation dynamics of molecular species, particularly determinations of the kinetic energies released upon dissociation, provide a stringent test for the reliability of contemporary quantal calculations of the shapes of potential-energy functions for various electronic states of such species. However, whereas considerable progress has been attained in developing powerful experimental probes of the dissociation dynamics of singly and multiply charged molecular ions by various photoionization techniques, such as photoelectron-photoion coincidence (PEPICO), photoion-photoion coincidence (PIPICO), photoelectron-photoion-photoion coincidence (PEPIPICO) [5], and more sophisticated variations such as electron-pair-ion coincidence (EPIC) [6], the application of such methods to studies of radical species continues to be problematic due to the difficulties of producing sufficient number densities of these inherently unstable species.

Such constraints are less important in ion-collision experiments in which sufficient quantities of radical ions can be created by electron impact on stable precursor molecules. We report here the results on one such series of collision-induced dissociation experiments on $S_2{}^+$ dimer ions and CS^+ radicals. The distributions of kinetic energies released upon dissociations $S_2{}^+ \rightarrow S^+ + S$, $CS^+ \rightarrow S^+ + C$, and $CS^+ \rightarrow C^+ + S$ in 3-keV collisions of the incident ions with neutral N_2 molecules have been measured using the ion-translational energy spectrometry technique. The experimental data is analyzed in conjunction with computer simulations of the energetics accompanying each dissociation process and distinct dissociation channels are identified.

II. EXPERIMENTAL METHOD

Our application of the ion-translational energy spectrometry technique to studies of the dissociation of doubly charged molecular species has been described in a number of recent reports [7]. A schematic diagram of the apparatus used in the present measurements is shown in Fig. 1.

Briefly, the apparatus comprises a high-pressure electron-impact ion source, a cylindrical electrostatic lens assembly to produce a collimated ion beam, a Wien filter to carry out analysis on the basis of mass-to-charge ratio, and a parallel-plate electrostatic energy monochro-

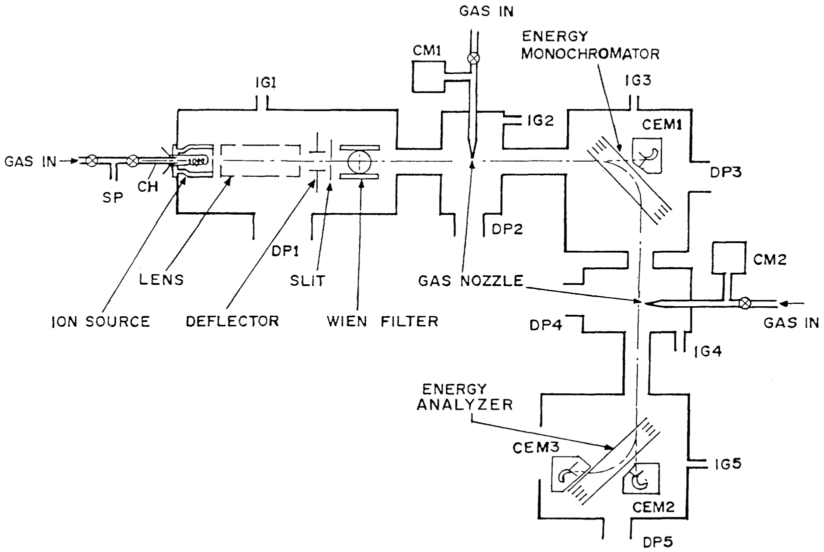

FIG. 1. Schematic diagram of the ion-translational energy spectrometer. DP1-5, diffusion pumps; IG1-5, ionization gauges; CEM1-3, channel electron multipliers; CM1-2, capacitance manometer heads for absolute pressure determination in the lines preceding the neutral gas jets (not used in the present studies); SP and CH, oil-free sorption pump and solid charge holder within the ion source assembly.

mator to produce a monoenergetic ion beam which intersects, in a 90° crossed-beam geometry, a gas jet of neutral target atoms or molecules. Forward-scattered collision products are energy analyzed by a second parallel-plate electrostatic energy analyzer. Ion detection is by means of a channel electron multiplier operating in the particle counting mode, coupled to conventional fast electronics and a multichannel analyzer. Typical gas pressures within the ion source are in the $1\times10^{-1}-5\times10^{-2}$-Torr range. Immediately outside the ion source and in the region of the energy analyzers and the detector, the pressure is maintained in the 10^{-7}-Torr range by means of fast differential pumping; in the collision region, the number densities in the neutral molecular beam correspond to pressures in the region of the 5×10^{-4}-Torr range.

A more detailed description of the apparatus has been presented elsewhere [8]; it is, however, pertinent to the present study to note the unusually high angular resolution ($0^\circ \pm 0.005^\circ$) for product-ion energy analysis in the present apparatus as this has a bearing on the dissociation spectra measured in this study. Implications of this aspect of our experimental design will be discussed in the context of the results presented below. At this juncture it is sufficient to draw attention to the fact that momentum transfer to the target ion in our collision systems is negligible; simple kinematics applied to our zero-degree scattering situation indicates that the recoil imparted to the target is ≤ 0.1 eV in the present measurements.

III. RESULTS AND DISCUSSION

A. Collision-induced dissociation of $S_2{}^+$ dimers

$S_2{}^+$ ions were formed in our high-pressure electron-impact ion source from CS_2 precursor molecules. From purely quantal considerations, it is clear that the lowest-energy $S_2{}^+$ formation process from CS_2 by a dissociative ionization process of the type

$$CS_2 \to S_2{}^+({}^2\Pi_g) + C({}^3P) + e$$

is forbidden by the spin-conservation rule. Although this rule may be circumvented in electron-impact situations by exchange processes near threshold, emission spectroscopy data [9] indicate that the potential energy curve of the ${}^2\Pi_g$ ground electronic state of $S_2{}^+$, with an equilibrium internuclear separation of 1.8 Å, would not be accessible in vertical transitions from the ground state of the linear CS_2 precursor in which the equilibrium distance between the two sulfur atoms is as large as 3.2 Å. Results of Hartree-Fock calculations [10] on low-lying electronic states of $S_2{}^+$ indicate that initial dimer ion formation may be into the lowest-energy ${}^6\Sigma$ state, whose potential-energy curve possesses a minimum in the region of 2.9-Å internuclear separation. Thereafter, radiationless transitions, aided by spin-orbit interactions, will lead to decay to the ${}^2\Pi_g$ ground electronic configuration.

Figure 2 shows the translational energy spectra of S^+ fragments obtained in 3-keV collisions of $S_2{}^+$ with a neutral N_2 beam. Three typical spectra are shown which have been accumulated under different ion-source conditions, corresponding to electron-impact energies of 43 eV, 70 eV, and 84 eV; the energy-analyzer voltage scale has been normalized with respect to the peaks obtained in each case. Careful examination indicates that all three spectra are identical, indicating that the high pressure of CS_2 within our ion source ensures effective collisional deactivation of any excited electronic dimer ion states that may initially be formed.

The halfwidth of each of the S^+ fragment-ion peaks shown in Fig. 2 is of the order of 50 V in terms of energy-analyzer voltage; the corresponding halfwidth for the elastically scattered $S_2{}^+$ peak was ca. 2 V. The broadening of the fragment ion peak is caused by the conversion of released dissociation energy into translational energy. Measurement of the halfwidth of the fragment-ion peak yields an incompletely defined *average* value of the center-of-mass kinetic energy released upon dissociation. If E is the kinetic energy of a projectile homonuclear di-

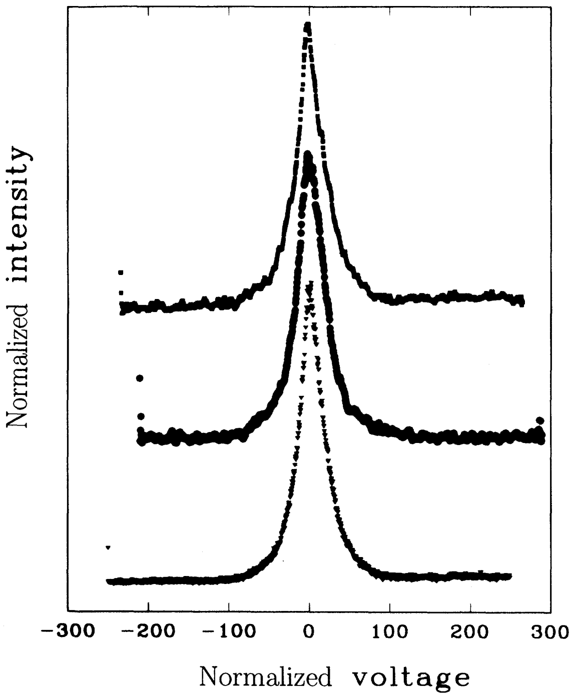

FIG. 2. Translational energy spectra of S^+ fragment ions produced in 3-keV collisions of $S_2{}^+$ with N_2. The lowest, middle, and uppermost curves were obtained with electron energies of 43 eV, 70 eV, and 84 eV, respectively, in the ion source. The abscissa represents the energy-analyzer voltage normalized to the peak of each curve.

atomic molecule and $K_{\text{c.m.}}$ is the kinetic energy released (in the center of mass) upon dissociation, the measured energy in the laboratory frame ϵ, can be deduced simply by the addition of collision velocities,

$$\epsilon = E/2 \pm (K_{\text{c.m.}}E)^{1/2} + K_{\text{c.m.}}/2. \quad (1)$$

An amplification of $K_{\text{c.m.}}$ in the laboratory frame occurs in this transformation process; it can be demonstrated most easily by considering a typical kinetic-energy release of 5 eV following dissociation of a homonuclear diatomic doubly charged molecule [7]. For an incident molecular-ion energy of 3 keV, the fragment ion possessing this value of kinetic-energy release will appear in the laboratory frame at 1500±245 eV; in practice, two peaks will be seen in the translational energy spectrum around 1500 eV, each separated from the other by 490 eV (corresponding to fragment ions which are forward and backward scattered ions in our high-angular-resolution apparatus). This energy "amplification" makes it possible to study dissociation processes even in instruments possessing relatively modest energy resolution capabilities.

In the case of dissociation of singly charged molecules, the values of $K_{\text{c.m.}}$ are considerably smaller, so that forward- and backward-scattered fragment-ion peaks possess sufficient intrinsic widths to coalesce into a single, broad peak. Although all three spectra shown in Fig. 2 are essentially devoid of any reproducible fine structure, careful examination of the peak shape does indicate the presence of more than a single-valued $K_{\text{c.m.}}$. In order to extract information on the different $K_{\text{c.m.}}$ components contributing to the overall width of the S^+ peak, we have carried out computer simulations of fragment-ion trajectories in our apparatus, for a given distribution of $K_{\text{c.m.}}$ components, in an attempt to reproduce the fragment-ion peak shapes actually observed in our translational energy spectra. The best agreement between the shapes of simulated and measured data is sought for the *minimum* number of $K_{\text{c.m.}}$ components in the fragment-ion beam.

The simulation is carried out in the following manner. The input to the post-collision energy analyzer is assumed to consist of groups of ions possessing a mixture of center-of-mass energies which are taken to be Gaussian distributions centered around distinct $K_{\text{c.m.}}$ values. The relative weight of each $K_{\text{c.m.}}$ component is an adjustable parameter. Ion trajectories through the energy analyzer are then computed for a range of parallel-plate voltages in small steps and the number of ions reaching the detector at each step is integrated. The distribution of entry angles of fragment ions into the analyzer can be chosen appropriately; in the present instance, the very high angular resolution of the apparatus enables us to calculate each trajectory for a fixed entry angle of 45°. All electrostatic fields in the apparatus are assumed to be ideal in the sense that field penetration and fringing effects are taken to be negligible. No magnetic fields are accounted for in the simulated ion trajectories.

Figure 3 shows typical results of tests carried out with our simulation program. In Fig. 3(a), peaks marked 1, 2, and 3 are the peak shapes obtained from simulated trajectories of ions containing one, two, and three $K_{\text{c.m.}}$ components traversing our apparatus. Peak 1 corresponds to the transmission of a molecular $S_2{}^+$ peak possesing only thermal energy (nominally taken to be 0 eV) in the center-of-mass frame. For such a single $K_{\text{c.m.}}$ component, the peak shape obtained as the ion emerges from the post-collision energy analyzer in our appartus is symmetrical to a very high order, in conformity with the measured shape of $S_2{}^+$ elastic-scattering peaks in our experiments. The addition of a 0.5-eV $K_{\text{c.m.}}$ component (peak 2) with a weight of 0.5 relative to the thermal energy component gives rise to a broadened peak shape. Addition of a third KER_{cm} component, of value 1.5 eV and a weight of 0.2 relative to the thermal energy component, gives rise to an even broader peak which exhibits a pronounced hump structure which is symmetrical about the central portion, representing forward- and backward-scattered components of 1.5-eV ions. It is pertinent to draw attention to the fact that almost perfect simulation of the shape of an elastically scattering peak in our translational energy spectrum can be accomplished with a single $K_{\text{c.m.}}$ component of 0 eV, as shown in Fig. 3(b); any "tailing" observed in measured inelastic peaks to be discussed subsequently are difficult to ascribe to purely instrumental factors connected with the transmission properties of our parallel-plate energy analyzer and must be attributed to large $K_{\text{c.m.}}$ components present in the ion beam.

Figure 4 shows comparisons between simulated S^+ fragment-ion spectra and measured data. Simulations have been carried out with two, three, and four $K_{\mathrm{c.m.}}$ components. In the case where only two $K_{\mathrm{c.m.}}$ components of 0 eV and 0.3 eV are used, the resulting S^+ peak is considerably narrower than that measured. Even the addition of a third, larger $K_{\mathrm{c.m.}}$ component of 2 eV does not yield as satisfactory a fit as is obtained when a fourth, intermediate-energy component of 1.5 eV is added. Figure 5 shows comparisons between simulated S^+ fragment-ion spectra and measured data acquired for two different electron energy values in the ion source. After a large number of simulations, with different numbers and relative weights of $K_{\mathrm{c.m.}}$ components, the best agreement between the measured shape and simulated spectra was obtained using the four $K_{\mathrm{c.m.}}$ components (0 eV, 0.3 eV, 1.5 eV, and 2.0 eV) occurring in relative weights 100:40:12:6. The existence of a low-energy group of $K_{\mathrm{c.m.}}$ values (0 eV and 0.3 eV) and a distinctly higher-energy group (1.5 eV and 2.0 eV) suggests that two different types of dissociation processes may be contributing. We discuss these in terms of the schematic potential-energy curves shown in Fig. 6.

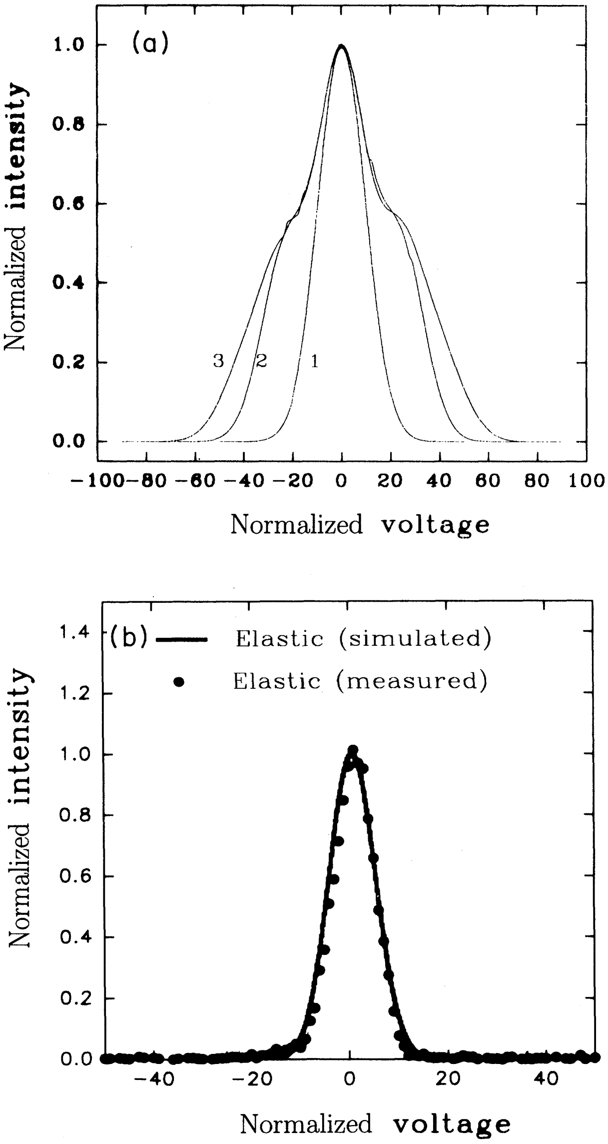

FIG. 3. Computer simulations of ion trajectories through the translational energy spectrometer. (a) Curves 1, 2, and 3 represent ion beams possessing center-of-mass kinetic-energy components of 0 eV, 0 eV + 0.5 eV, and 0 eV + 0.5 eV +1.5 eV, respectively. (b) The dots represent the measured peak shape of elastically scattered $S_2{}^+$ ions in 3-keV collisions with He, and the solid line is the corresponding simulated peak shape with a single center-of-mass kinetic-energy component of 0 eV.

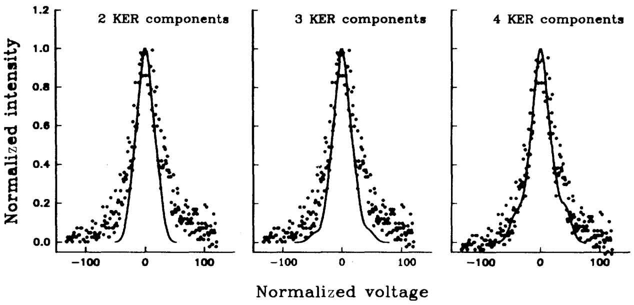

FIG. 4. Comparison of experimental (dots) and simulated (line) translational energy spectra of S^+ fragments from collision-induced dissociation of $S_2{}^+$ ions. K refers to center-of-mass kinetic-energy release. Two K components are 0 eV and 0.3 eV; three K components: 0 eV, 0.3 eV, and 2.0 eV; four K components: 0 eV, 0.3 eV, 1.5 eV, and 2.0 eV.

The low-energy components are postulated to occur via a curve-crossing mechanism involving an excited bound state of $S_2{}^+$ and a repulsive state which has a dissociation limit S^+ (^2D) + S (^3P), as shown in Fig. 5(a). $K_{\mathrm{c.m.}}$ values of 0 eV and 0.3 eV are indicative of predissociation of two vibrational levels of the $S_2{}^{+*}$ bound-state curve. Although paucity of theoretical information on electronically excited states of $S_2{}^+$ precludes a more precise quantal identification of the states at present it appears reasonably certain that a curve-crossing process involving a lower-energy bound state $S_2{}^+$ curve leading to the ground state S^+ (^4S) + S (^3P) limit would be unlikely to give rise to $K_{\mathrm{c.m.}}$ values which are as small as 0 eV.

In the case of the higher-energy $K_{\mathrm{c.m.}}$ components, we postulate direct collision-induced dissociation of the type shown in Fig. 6(b). The electronic configuration of the ground electronic state $(^2\Pi_g)$ of $S_2{}^+$ [10] can be written as

$$(\mathrm{core})^{20} 1\sigma_g^2 1\sigma_u^2 2\sigma_g^2 1\pi_u^4 1\pi_g .$$

Collisional excitation of an electron from the outermost $1\pi_g$ orbital to higher-lying, nonbonding $d\sigma$ and $d\pi$ orbitals will give rise to states possessing overall symmetries such as $^2\Delta$ and $^2\Phi$ which have purely repulsive potential-energy curves dissociating to the lowest-energy S^+ (^4S) + S (^3P) limit. As in the case depicted in Fig. 6(a), there is no quantum-chemical information available on the potential-energy curves of such $S_2{}^{+*}$ states at present; however, it is not unreasonable to postulate that dissociation of $S_2{}^+$ along the $^2\Delta$ and $^2\Phi$ potential curves will be expected to release kinetic-energy values which lie in the 1–2-eV range.

B. Collision-induced dissociation of CS^+ radicals

The translational energy spectra of S^+ fragment ions from collision-induced dissociation of CS^+ shows a broad peak with symmetrical fine structure on either side of the center. A large number of experimental runs were carried out under varying collision gas pressure and ion-source conditions to ensure reproducibility of the fine structure. Indeed, preliminary evidence for such a structure was also forthcoming in the earlier study of Krishnamurthi *et al.* [7], although deconvolution procedures had to be resorted to in that case because of energy resolution and sensitivity constraints. Figure 7 shows two typical spectra measured at different values of gas pressure in the collision zone. Three pairs of peaks, identified in the figure as *a*-*a*′, *b*-*b*′, and *c*-*c*′, are clearly visible; a careful examination of all the measured spectra indicates that additional, higher-energy, $K_{\text{c.m.}}$ components are also present which account for the tailing on either side of the peak.

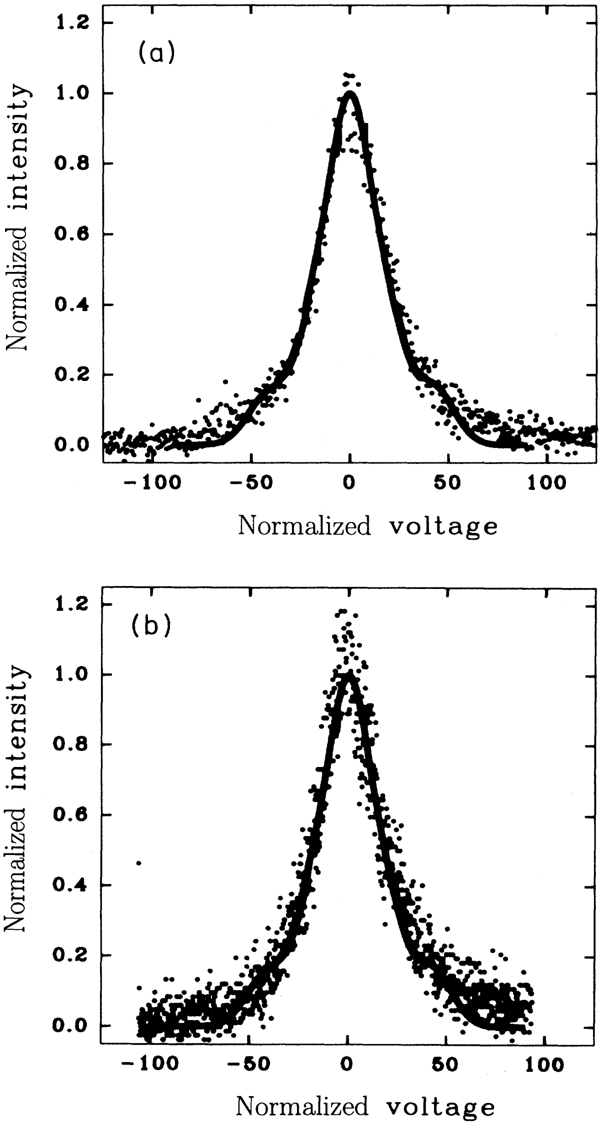

FIG. 5. Comparison of experimental (dots) and simulated (line) translational energy spectra of S^+ fragments from collision-induced dissociation of $S_2{}^+$ ions under different ion-source conditions: (a) 70-eV electron energy; (b) 84-eV electron energy. The simulated curves are for center-of-mass kinetic-energy release values of 0 eV, 0.3 eV, 1.5 eV, and 2.0 eV, in relative weights 100:40:12:6.

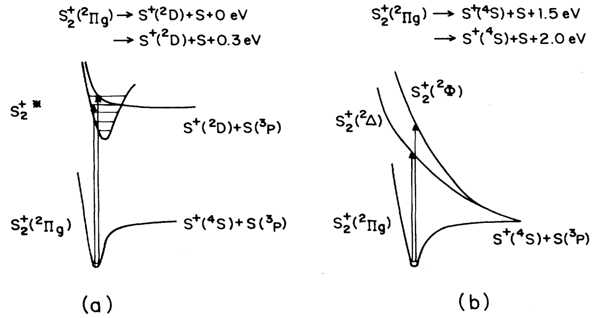

FIG. 6. Schematic potential-energy curves depicting different dissociation processes occurring in the $S_2{}^+ \rightarrow S^+$ fragmentation (see text).

Conversion of the laboratory energies of fine structures *a*–*c* in a number of spectra indicate the presence of $K_{\text{c.m.}}$ components having values of 39±9 meV, 66±5 meV, and 106±4 meV. In addition, our ion-trajectory simulation studies indicate that at least three higher-energy components, having $K_{\text{c.m.}}$ values of 3.5 eV, 5 eV, and 7 eV, have to be invoked in order to account for the tailing observed on the low-energy and high-energy sides of the S^+ peak. The latter group of large $K_{\text{c.m.}}$ values is explainable in terms of a direct dissociation mechanism, involving initial excitation to purely repulsive CS^{+*} electronic states lying up to 7 eV vertically above the lowest vibrational level of the $^2\Sigma^+$ ground state. The relatively high values of $K_{\text{c.m.}}$ are a consequence of the breaking of a $C{\equiv}S$ triple bond which is very strong. On the other hand, the former group of small $K_{\text{c.m.}}$ values are difficult to account for within the framework of the dissociation mechanisms depicted schematically in Fig. 6. In an earlier report of lower-resolution experiments on the dissociation of CS^+, Krishnamurthi *et al.* [7] considered the most obvious interpretation involving predissociation of higher vibrational levels of the $C\,^2\Sigma$ state of CS^+ by a repulsive state of either $^4\Sigma$ or $^2\Pi$ symmetry. On the basis of the present data, we are inclined not to favor this interpretation. Typical vibrational spacings of any excited electronic state of CS^+ (including the $C\,^2\Sigma$ state) which might be involved in a predissociation process would be larger (ca. 180 meV) than the measured fine-structure separations. On the other hand, multiplet structure at the C ($^3P_{2,1,0}$) + S^+ (^{4}S) dissociation limit would give rise to considerably smaller $K_{\text{c.m.}}$ values. The $K_{\text{c.m.}}$ values that have been measured in the present experiments lead us to postulate dissociation of *rotationally excited* CS^+ ions, with a', b', and c' representing the forward-scattered ions and a, b, and c representing the backward-scattered components.

The importance of high rotational angular-momentum states in determining photodissociation cross sections for diatomic molecules has long been appreciated in studies on molecular formation and destruction processes in interstellar space [11]. For rotationally hot diatomic molecules, the addition of the extra centrifugal energy term

$$V_{\rm rot}(r) = \hbar^2 J(J+1)/2\mu r^2 \qquad (2)$$

to the rotationless ground-state potential-energy function gives rise to an *effective* potential-energy curve with a rotational barrier at large values of internuclear spearation r. For a range of values of the rotational quantum number J, there will exist vibrational levels in the effective potential-energy curve which lie *above* the ground-state dissociation limit. These quasibound rotational resonance states decay by tunneling through the potential barrier, their lifetimes being determined by the barrier shape and the reduced mass of the quasibound system [12]. In the present experiments, the absence of any S^+ fragment-ion signal without an adequate pressure of collision gas indicates that the rotational excitation is entirely induced by the 3-keV collision of ground-state CS^+ with neutral N_2. Due to the acute paucity of experimental information on cross sections for rovibronic excitation in fast collisions between molecular ions and neutral atoms and molecules, it is, unfortunately, difficult to be more than speculative on this matter at present. It must, however, be noted that of the possible large number of rotationally excited quasibound states which may be energetically accessible in the present experiments, only a subset will actually be detected because of considerations of the lifetimes of the resonance states. Comprehensive discussions have been presented before on the constraints that an experimental lifetime window places on studies of quasibound states by means of translational energy spectrometry and momentum spectrometry [13].

Figure 8 shows a typical translational energy spectrum of C^+ fragments resulting from 3-keV collisions of CS^+ with N_2. The signal intensities from this dissociation channel were found to be at least one order of magnitude lower than for the case of S^+ formation. The overall width of the fragment-ion peak is considerably less than the corresponding S^+ peak, indicating that much lower $K_{\rm c.m.}$ values are obtained in this dissociation chan-

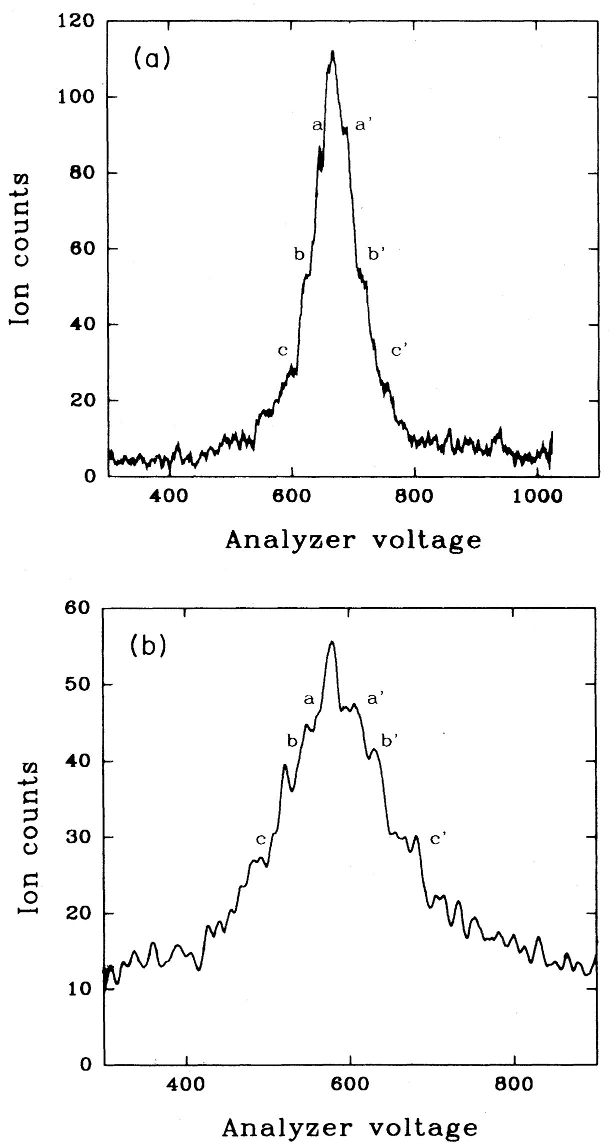

FIG. 7. Translational energy spectra of S^+ fragments from collision-induced dissociation of CS^+ ions in collisions with N_2 measured at different collision gas pressures: (a) 8×10^{-6} Torr, (b) 2×10^{-6} Torr.

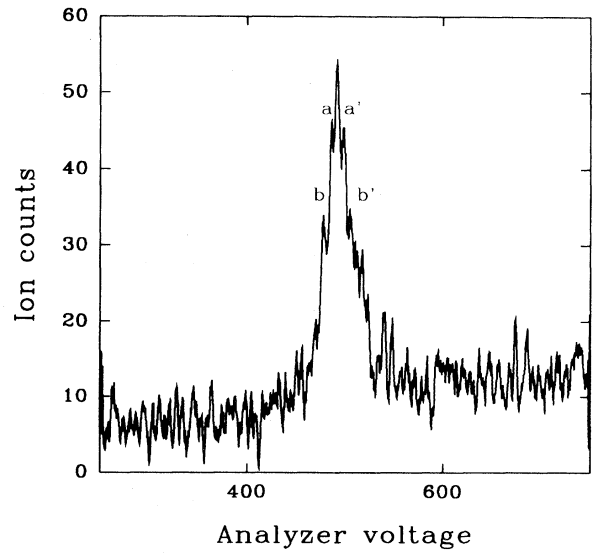

FIG. 8. Translational energy spectrum of C^+ fragments from collision-induced dissociation of CS^+ ions in 3-keV collisions with N_2.

nel. The relatively poor signal-to-noise ratios that were obtained in our experiments precluded meaningful comparisons with computer simulations of C^+ trajectories. However, symmetrical structures marked *a-a′* and *b-b′* in Fig. 8 were observed in measurements carried out at different pressures in the collision region; they represent $K_{\rm c.m.}$ values of 51 meV and 270 meV, respectively.

IV. SUMMARY

Collision-induced dissociation experiments on S_2^+ dimer ions and CS^+ radicals have been carried out by means of the ion-translational energy spectrometry using a crossed-beams apparatus possessing a very high angular resolution ($\leq 10^{-4}$ rad). The initial ion production process takes place in a high-pressure ion source within which collisional deexcitation occurs very efficiently such that both S_2^+ and CS^+ projectile beams comprise ions which are essentially in their respective ground electronic states.

The distributions of kinetic energies released upon dissociations $S_2^+ \rightarrow S^+ + S$, $CS^+ \rightarrow S^+ + C$, and $CS^+ \rightarrow C^+ + S$ in 3-keV collisions of the incident ions with neutral N_2 molecules have been measured; computer simulations of trajectories through the translational energy spectrometer of ions possessing different center-of-mass kinetic-energy release ($K_{\rm c.m.}$) components have also been carried out to aid interpretation of the shapes of the translational energy spectra of fragment ions.

In the case of S^+ formation from S_2^+ dimers, dissociation occurs via excitation to S_2^{+*} electronic states with purely repulsive potential curves, giving rise to $K_{\rm c.m.}$ components of 1.5 eV and 2.0 eV; lower $K_{\rm c.m.}$ values (0 eV and 0.3 eV) are obtained as a result of dissociation of a bound excited state of S_2^+ by a curve-crossing mechanism. In the case of CS^+, dissociation into $S^+ + C$ occurs via rotational resonances, giving rise to the narrow, symmetrical structure in the S^+ translational energy spectrum; direct dissociation also occurs which yields relatively high values of $K_{\rm c.m.}$ as high as 7 eV due to the breaking of the strong $C\equiv S$ triple bond. The $CS^+ \rightarrow C^+ + S$ dissociation channel produces signal intensities which are more than one order of magnitude weaker than for the S^+ formation channel.

ACKNOWLEDGMENTS

We are grateful to F. A. Rajgara and Vidhya Krishnamurthi for assistance with the experimental apparatus and to M. Krishnamurthy and E. Krishnakumar for very useful discussions.

[1] M.F. A'Hearn and P.D. Feldman, in *Ices in the Solar System*, edited by J. Klinger, D. Benesat, A. Dollfus, and R. Smoluchouski (Reidel, Dordrecht, 1985), p. 463; C. B. Cosmovici and S. Ortolani, Nature **310**, 122 (1984); C.B. Cosmovici, C. Barbieri, C. Bonoli, F. Bortoletto, and E. Hamzaoglu, Astron. Astrophys. **114**, 373 (1982); *Astrochemistry*, edited by M.S. Vardya and S.P. Tarafdar (Reidel, Dordrecht, 1985), and references therein.

[2] N. Jonathan, A. Morris, M. Okuda, D.J. Smith, and K.J. Ross, Chem. Phys. Lett. **13**, 334 (1972); D.C. Frost, S.T. Lee, and C.A. McDowell, *ibid.* **17**, 153 (1972).

[3] J. Baker, M. Barnes, M.C.R. Cockett, J.M. Dyke, A.M. Ellis, M. Feher, E.P.F. Lee, A. Morris, and J. Zamanpour, J. Electron. Spectrosc. Related Phenom. **51**, 487 (1990).

[4] W. Domcke, L. S. Cederbaum, W. von Niessen, and P. Kramer, Chem. Phys. Lett. **43**, 258 (1976); J. Schirmer, W. Domcke, L.S. Cederbaum, and W. von Niessen, J. Phys. B **11**, 1901 (1978).

[5] J.H.D. Eland, in *Vacuum Ultraviolet Photoionization and Photodissociation of Molecules and Clusters*, edited by C.-Y. Ng (World Scientific, Singapore, 1991).

[6] J.H.D. Eland and D. Mathur, Rapid Commun. Mass Spectrom. **5**, 475 (1991).

[7] V.R. Marathe and D. Mathur, in *Physics of Ion Impact Phenomena*, edited by D. Mathur (Springer-Verlag, Berlin, 1991), Chap. 8; D. Mathur, Phys. Rep. **225**, 193 (1993); V. Krishnamurthi, M. Krishnamurthy, V.R. Marathe, and D. Mathur, J. Phys. B **25**, 5149 (1992); K. Nagesha, V.R. Marathe, and D. Mathur, Chem. Phys. **154**, 125 (1991); D. Mathur, K. Nagesha, and V.R. Marathe, Chem. Phys. Lett. **200**, 394 (1992).

[8] D. Mathur, F.A. Rajgara, and V. Krishnamurthi, Proc. Indian Acad. Sci. (Chem. Sci.) **104**, 509 (1991).

[9] A.J. Capel, J.H.D. Eland, and R.F. Barrow, Chem. Phys. Lett. **82**, 496 (1981).

[10] S. Mazumdar, S.V.K. Kumar, V.R. Marathe, and D. Mathur, Rapid Commun. Mass Spectrom. **3**, 24 (1989).

[11] S.J. Singer, K.F. Freed, and Y.B. Band, Chem. Phys. Lett. **105**, 158 (1984); M.M. Graff and J.T. Moseley, *ibid.* **105**, 163 (1984), and references therein.

[12] V. Krishnamurthi, D. Mathur, and G.T. Evans, Rapid Commun. Mass Spectrom. **5**, 557 (1991).

[13] A.G. Brenton, J.H. Beynon, E.G. Richard, and P.G. Fournier, J. Chem. Phys. **79**, 1834 (1983); R. Locht, J.G. Maas, N.P.F.B. Van Asselt, and J. Los, Chem. Phys. **15**, 179 (1976).